metrologia

Ultra-precise thermal expansion measurements of ceramic and steel gauge blocks with an interferometric dilatometer

M. Okaji, N. Yamada and H. Moriyama

Abstract. Linear thermal expansion coefficients (LTECs) of two kinds of ceramic gauge block (seven in all) and steel gauge blocks (four in all) were measured in the range –10 °C to 60 °C with an optical heterodyne interferometric dilatometer. The dilatometer has an uncertainty and reproducibility of the order of 1×10^{-9} K^{-1} in LTEC measurements. LTECs of $(9.229 \pm 0.011) \times 10^{-6}$ K^{-1} were obtained for four 2 % Al_2O_3 partially stabilized zirconia (PSZ) gauge blocks; $(9.381 \pm 0.003) \times 10^{-6}$ K^{-1} for three 99.9 % PSZ gauge blocks; and $(10.702 \pm 0.064) \times 10^{-6}$ K^{-1} for four steel gauge blocks. These results are discussed in relation to the compositions and production batches of the gauge blocks.

1. Introduction

Reliable thermal expansion data are necessary to maintain length standards in precision engineering, especially for dimensional measurements. Knowledge of the linear thermal expansion coefficient (LTEC) is essential in order to correct the absolute length of gauge blocks, and to compare dimensional measurements at different reference temperatures. Several papers have been published relating to thermal expansion measurements of gauge blocks [1-4], and to international comparisons of short and long gauge-block measurements among the national measurement institutes of EUROMET [5, 6].

As a contribution to dimensional metrology, we have developed an interferometric dilatometer that operates at room temperature [7, 8]. This dilatometer, comprising a double-path interferometer with sub-nanometre accuracy in optical fringe determination, and using the optical heterodyne technique and a compact vacuum thermal bath controlled by a thermoelectric transducer, allows accurate and efficient measurements. We have previously presented details of the dilatometer with measurement results for several kinds of reference material, such as copper, tungsten, fused silica supplied by the National Institute of Standards and Technology (NIST), and a high-purity single crystal of silicon [7, 8]. The LTECs of these materials show extremely good agreement with the NIST measured values [9-11] and the CODATA recommended data [12] in the measured temperature range.

This work presents the measured LTECs of steel gauge blocks and two kinds of ceramic gauge blocks (made from "pure" partially stabilized zirconia (PSZ), or PSZ including 2 % Al_2O_3), in the temperature range –10 °C to 60 °C. All the blocks are 100 mm long. The scatter of the measured LTEC values from a polynomial fitting curve was about 1×10^{-9} K^{-1}. The reproducibility of the measurements was similar for all the gauge blocks. The differences among the LTECs of these gauge blocks are discussed, together with their compositions and production batches.

2. Apparatus

The interferometric dilatometer consists of three main parts: a double-path interferometer, a vacuum thermal bath, and a measuring instrument.

2.1 Double-path interferometer

Figure 1 is a schematic diagram of the double-path interferometer. Optical heterodyne interferometry is used to measure the change in length of the gauge block. Any non-linearity is avoided by means of two acousto-optical modulators (AOMs) that generate a beat frequency for the heterodyne interferometry. The uncertainty in the fringe determination is less than 1 nm. Details of the interferometer are given in our previous papers [7, 8].

M. Okaji and N. Yamada: Cryogenic Materials Section, Thermophysical Metrology Department, National Research Laboratory of Metrology (NRLM), 1-1-4 Umezono, Tsukuba, Ibaraki 305-8563, Japan. e-mail: okaji@nrlm.go.jp; tel: 81-298-61-4166; fax: 81-298-61-4039 http://www.nrlm.go.jp/section/Teion/index_j.htm
H. Moriyama: Mitutoyo Corporation, Tano-cho 10652-1, Miyazaki-gun, Miyazaki-pref. 889-1701, Japan.

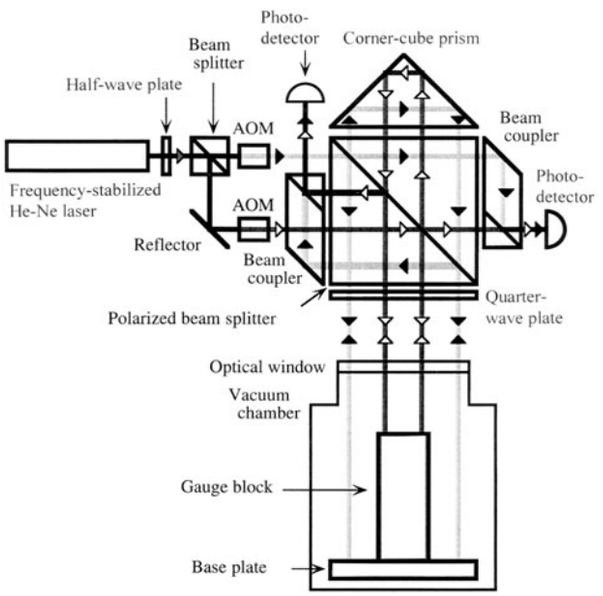

Figure 1. Schematic of the double-path interferometer.

2.2 Vacuum thermal bath

Figure 2 shows a compact vacuum thermal bath, specially constructed for the present work. This bath, driven by a thermoelectric transducer, covers the temperature range –10 °C to 60 °C. A temperature stability of 1 mK can be achieved after sufficient holding time. This type of bath has already been successfully applied to the measurement of thermal expansivity of some reference materials [7, 8]. However, the bath has previously been available only for "short" specimens, of maximum length 20 mm. For the present work, we rebuilt the vacuum chamber to accommodate much longer specimens, of up to 100 mm. The air-cooled thermoelectric transducer was also replaced by a water-cooled version in order to obtain greater driving power. The surface of the double thermal shield was gold-plated to produce a high reflection ratio. For the same reason, the inner surface of the vacuum chamber was polished. Another modification was to add a temperature controller for the optical window. The temperature of the optical window was kept constant at (20±0.05) °C to avoid excess uncertainty in the optical path length. The bath was evacuated to much less than 0.1 Pa (about 1×10^{-3} Torr) by an oil-free dry-scroll vacuum pump.

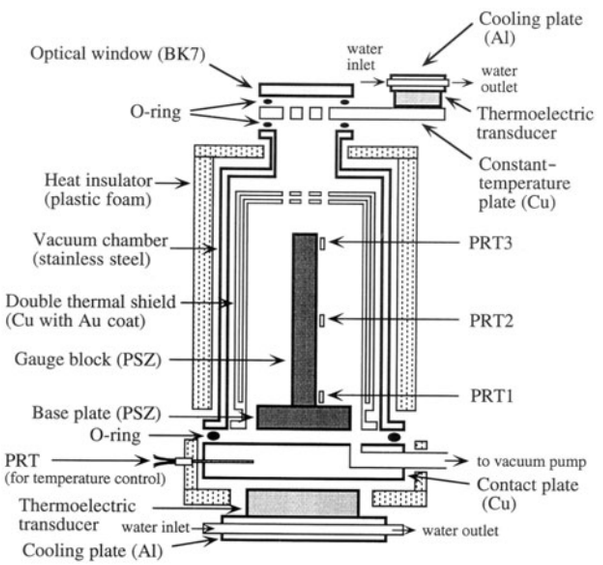

Figure 2. Mechanical arrangement of the vacuum thermal bath.

2.3 Measurement system

Figure 3 is a block diagram of the present measurement system. A single frequency-stabilized He-Ne laser (Melles-Griot 05STP901, output power 1.5 mW) was used as the light source. The reference and interference signals from the interferometer were both introduced into the lock-in amplifier. This system easily achieves sub-nanometre resolution in fringe detection.

Three platinum resistance thermometers (PRTs) (industrial grade Pt 100, Netsushin, NR251-1537-100S; 1.5 mm × 3 mm × 7 mm) were used for the gauge temperature measurements. The PRTs were calibrated with an uncertainty of 10 mK at temperatures of 0 °C, 50 °C, and 100 °C. A four-wire circuit was used to measure each PRT with a constant-current dc power source, the stability of which was confirmed to be better than 5 parts in 10^6 per day. Self-heating of the PRTs was checked using three different levels of the input electric current. Figure 4 shows the degree of self-heating and the noise level for the three current inputs through the PRT when the bath temperature was set at 60 °C. The degree of self-heating was confirmed to be almost constant over the temperature range –10 °C to 60 °C. As a result of these tests, a current of 0.3 mA was chosen for all the measurements.

2.4 Definition of linear thermal expansion coefficient and measurement uncertainty

The linear thermal expansion coefficient (LTEC) at a temperature T is defined as

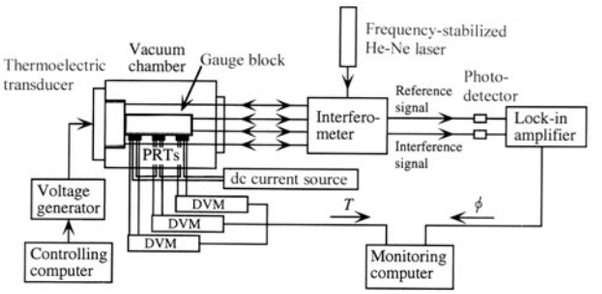

Figure 3. Block diagram of the dilatometric measurement system. DVM: digital voltmeter; T: temperature; ϕ: phase change.

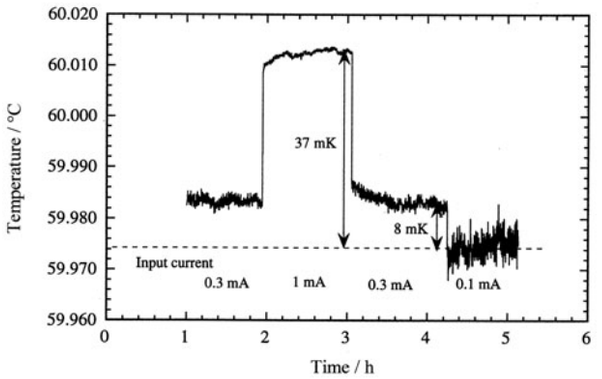

Figure 4. Self-heating of the PRTs for the three different input electric currents at 60 °C.

$$\alpha(T) = \mathrm{d}L/(L_0 \mathrm{d}T), \tag{1}$$

where $\mathrm{d}L$ is the infinitesimal change in the length of the material induced by an infinitesimal change $\mathrm{d}T$ in its temperature T, and L_0 is the length of the material at some reference temperature (usually 20 °C). However, the dilatometric measurement was actually carried out in the finite temperature interval $\Delta T = (T_2 - T_1)$ such that the mean LTEC defined by

$$\overline{\alpha}(\overline{T}) = \Delta L/(L_0 \Delta T) \tag{2}$$

was measured. Here, $\Delta L = L_2 - L_1$ and $\overline{T} = (T_1 + T_2)/2$. Generally, $\overline{\alpha}(\overline{T})$ differs slightly from $\alpha(T)$. The difference depends on the magnitude of ΔT (10 °C in the present experiment) and the temperature dependence of the LTEC. The difference between $\alpha(T)$ and $\overline{\alpha}(\overline{T})$ was calculated as described in [13] to be 3×10^{-10} K^{-1} at most. This value is considered negligibly small compared with the other uncertainties in the present work.

The sources of dilatometer uncertainty are laser wavelength instability, fringe determination, long-term interferometer instability, temperature determination, temperature instability, and the PRT calibration. Table 1 summarizes estimates of these uncertainties. The expanded total uncertainty $(k = 2)$ of the measurement system is calculated to be 7×10^{-9} K^{-1} under our measurement conditions: $L_0 = 100$ mm and $\Delta T = 10$ °C.

Table 1. Performance of the dilatometer for a 100 mm gauge and a 10 °C interval.

Element	Uncertainty	Uncertainty contribution to LTEC/K^{-1}
Length measurement		
Laser wavelength instability	2×10^{-9}	2×10^{-10}
Fringe determination	0.5 nm	5×10^{-10}
Long-term interferometer instability	< 5 nm/100 h (0.35 nm/7 h)	3.5×10^{-10}
Temperature measurement		
Temperature determination	1 mK	1×10^{-9}
Temperature instability	1 mK	1×10^{-9}
PRT calibration	10 mK over 50 K	2×10^{-9}
Total uncertainty $(k = 1)$		3.6×10^{-9}
Expanded total uncertainty $(k = 2)$		7×10^{-9}

3. Gauge blocks

Two kinds of ceramic PSZ gauge block (seven in all: A1 to A4 and B1 to B3) were prepared. PSZ normally includes 5.3 % Y_2O_3 as a stabilizer, because inherent structural instability occurs with pure zirconia (ZrO_2). Gauges A1 to A4 include 2 % Al_2O_3 and gauges B1 to B3 are made from "pure" PSZ (99.9 % purity). Steel gauge blocks (four in all: S1 to S4) were also prepared. The dimensions of all gauge blocks were 9 mm × 35 mm × 100.000 mm.

Tables 2 and 3 summarize the specifications of the gauge blocks. The first two digits of the serial number represent the year of manufacture. Gauges A3 and A4 were cut from the same batch of raw material. Gauges A1 to A4 are commercially available from the Mitutoyo Corporation, made using ceramic powder from the same

Table 2. Specifications of the ceramic gauge blocks.

Gauge block	Serial no.	100 × Mass fraction			Source	Remarks
		PSZ*	Al_2O_3	Other		
A1	911879	≥ 97.83	2.1	≥ 0.07	X	
A2	950224	≥ 97.83	2.1	≥ 0.07	X	
A3	970209	≥ 97.83	2.1	≥ 0.07	X	Same batch
A4	970236	≥ 97.83	2.1	≥ 0.07	X	Same batch
B1	980001	99.90	0.075	0.025	Y	Same batch
B2	980002	99.90	0.075	0.025	Y	Same batch
B3	980003	99.90	0.075	0.025	Y	Same batch

*5.3 % Y_2O_3-ZrO_2.

Table 3. Specifications of the steel gauge blocks (nominal values).

Gauge block	Serial no.	100 × Mass fraction								Source
		C	Si	Mn	P	S	Cr	W	Fe	
S1	944263	2 to 2.2	≥ 0.4	≥ 0.5	≥ 0.025	≥ 0.02	12 to 13	0.7 to 1.0	Balance	Z
S2	966153	2 to 2.2	≥ 0.4	≥ 0.5	≥ 0.025	≥ 0.02	12 to 13	0.7 to 1.0	Balance	Z
S3	974560	2 to 2.2	≥ 0.4	≥ 0.5	≥ 0.025	≥ 0.02	12 to 13	0.7 to 1.0	Balance	Z
S4	986329	2 to 2.2	≥ 0.4	≥ 0.5	≥ 0.025	≥ 0.02	12 to 13	0.7 to 1.0	Balance	Z

manufacturer. Gauges S1 to S4 are also commercially available from the Mitutoyo Corporation. Gauges B1 to B3, however, were prototypes made from ceramic powder from another source.

4. Interferometric measurements

The gauge was attached to a base plate made from the same material, 40 mm in diameter and 20 mm thick. In the case of the ceramic gauges, the base plate, except where it was in contact with the gauge, and the top surface of the gauge, were coated in a thin film of aluminium for high reflectivity of the laser beam.

All dilatometric measurements were made by temperature cycling over an operating range from –10 °C to 60 °C. Each measurement cycle involved attaching individual gauges to the base plate. The mean LTECs ($\overline{\alpha}(\overline{T})$, see (2)) for the gauge blocks were determined at equal temperature intervals of 10 °C. The temperature at a given step was held for 7 hours. The heating and cooling rates between the two equilibrium temperatures were +0.5 °C/min and –0.5 °C/min, respectively. The total time for one experimental run was 105 hours (about 4.5 days). All gauges were measured over two cycles with re-wringing. The two individual LTEC values from the two runs show very good agreement with each other for all gauge blocks, with reproducibility better than 3×10^{-9} K^{-1}. The agreement is of the same order as the total estimated uncertainty (see Table 1).

5. Results

5.1 Temperature gradient and measurement settling time

Figure 5 shows a typical temperature gradient along the ceramic and steel gauge blocks in the longitudinal direction. The temperature gradient was measured by the three PRTs (PRT1, PRT2 and PRT3 in Figure 2) attached by high-vacuum grease to the side surface of the gauge. T_1, T_2, and T_3 are the temperatures at 5 mm from the bottom, the midpoint and 5 mm from the top, respectively, of the gauge.

In the case of the ceramic gauges, the differences between T_1 and T_3, and T_1 and T_2, reach 90 mK and –70 mK, respectively, at 60 °C, and –80 mK and 50 mK at –10 °C. Principal contributors to this gradient may be the external radiation entering the bath through the holes at the top of the thermal shield, and the temperature gradient of the thermal shield itself.

In the case of the steel gauges, the temperature differences $T_1 - T_2$ and $T_3 - T_2$, decreased to 30 mK and –20 mK at 60 °C, and –30 mK and 15 mK at –10 °C under the same measurement conditions. The temperature distributions are one-third to one-quarter smaller than those for the ceramic gauges, due to the higher thermal conductivity of steel. These temperature

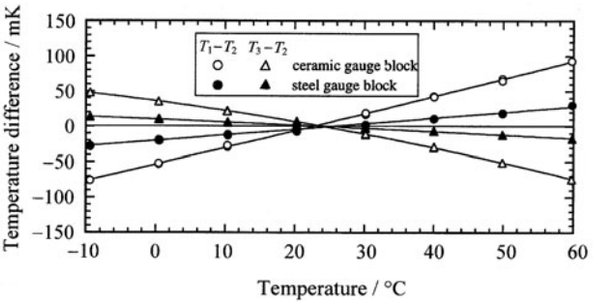

Figure 5. Typical temperature distribution along the specimen in the longitudinal direction. ○ and ● represent $T_1 - T_2$, and Δ and ▲ represent $T_3 - T_2$, for ceramic and steel gauges, respectively.

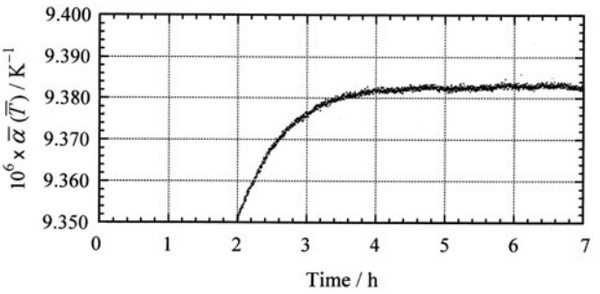

Figure 6. Example of settling behaviour and noise level for an experimental run of ceramic gauge block A1.

distributions were very reproducible, within a few millikelvin, through all the experimental runs. The temperature gradient along the gauges contributes to the measurement uncertainty, because the LTEC is a function of temperature. However, the effect of the temperature gradient on the LTEC was estimated to be less than 3×10^{-9} K^{-1} even in the case of the maximum temperature gradient (see Figure 5). In addition, a correction can be made based on the temperature distribution measured using the three PRTs attached to the gauges.

Figure 6 shows part of a typical measurement for ceramic gauge block A1 as a function of time after stepwise temperature changes of the thermal bath from 30 °C to 40 °C. Since the LTEC approaches a constant value of the order of 1×10^{-9} K^{-1} within 5 hours, 7 hours is an adequate delay to allow for temperature stabilization of the ceramic gauges at each step. Roughly 3 hours is enough to settle the LTEC value for the steel gauges. The amount of scatter of the individual data points recorded every 10 s is also of the order of 1×10^{-9} K^{-1}.

5.2 Linear thermal expansion coefficients

Figure 7 gives an example of LTEC data for an experimental run with gauge block A2. The standard deviation of individual data points from the second-order polynomial fitting function is about 1×10^{-9} K^{-1} in this run.

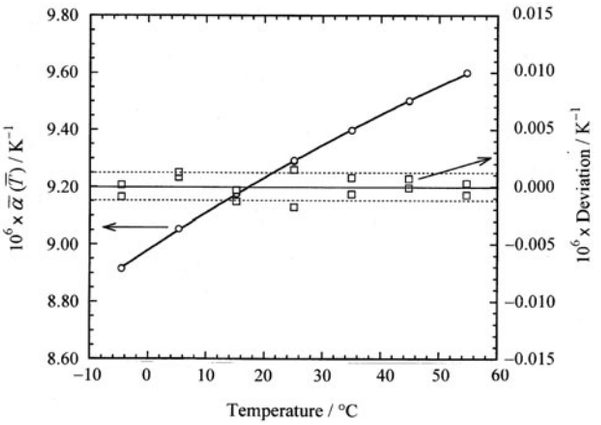

Figure 7. Measured linear thermal expansion coefficient and data scatter for gauge block A2. The dashed lines represent the standard deviation, 1×10^{-9} K^{-1}, of the data points from the second-order fitting function.

The coefficients of the polynomial fitting functions of the LTECs for all gauge blocks in the temperature range –5 °C to 55 °C were calculated. The residual errors were confirmed to be almost the same for second- and third-order polynomial functions for both ceramic and steel gauge blocks. Thus, we calculated the $\alpha(T)$ values using the following function:

$$\alpha(T) = c_0 + c_1(T-20) + c_2(T-20)^2. \qquad (3)$$

Table 4 lists all the calculated coefficients. Coefficient c_0 differs from gauge to gauge, while coefficients c_1 and c_2 are almost unchanged for all the ceramic gauges. Similar behaviour occurs with coefficients c_0 and c_1, but coefficient c_2 varies among the steel gauges. Figures 8a and 8b show the generated LTECs from the measurement of the two kinds of ceramic and the steel gauge blocks, respectively, from –5 °C to 55 °C.

6. Discussion

Figure 9a shows the LTECs at 20 °C for the two kinds of ceramic gauge block, and Figure 9b shows those for the steel gauge blocks. The error bars represent the standard deviation of individual data points from the second-order polynomial fit in the range –5 °C to 55 °C (see Figure 7).

Table 4. Polynomial coefficient of the linear thermal expansion coefficients for the gauge blocks; $\alpha(T) = c_0 + c_1(T-20) + c_2(T-20)^2$.

	Coefficient		
Gauge block	$10^6 \times c_0$/K^{-1}	$10^6 \times c_1$/K^{-2}	$10^{11} \times c_2$/K^{-3}
A1	9.2418	0.011 790	–3.5933
A2	9.2322	0.011 789	–3.8608
A3	9.2253	0.011 789	–3.7026
A4	9.2171	0.011 772	–3.8773
B1	9.3813	0.011 652	–3.7650
B2	9.3787	0.011 788	–4.1861
B3	9.3836	0.011 661	–3.7702
S1	10.770	0.013 206	–2.4831
S2	10.676	0.012 998	–2.2940
S3	10.737	0.013 141	–1.5051
S4	10.626	0.012 880	–1.4117

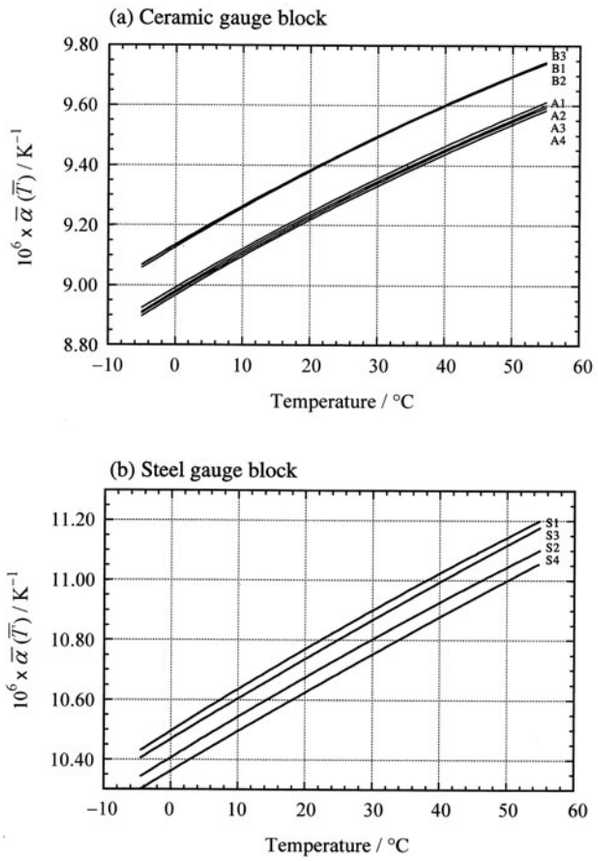

Figure 8. Generated values of the linear thermal expansion coefficients from the fitting functions for: (a) the two types of ceramic gauge block; (b) the steel gauge blocks.

The scatters of the LTECs among the four gauges A1 to A4 are 25×10^{-9} K^{-1}, which may indicate differences between different batches of the material. The differences seem to be small, however, even though the gauges were made over a six-year period. As mentioned above, gauges A3 and A4 were made from the same ceramic block; the small difference between them, 8×10^{-9} K^{-1}, suggests a small variation in the thermophysical characteristics of the raw material. There are also similar differences, about 5×10^{-9} K^{-1}, for the three gauges B1 to B3, made from a common batch. On the other hand, the differences for the four gauges S1 to S4 were 0.14×10^{-6} K^{-1}, which is about six times larger than those for the ceramic gauges A1 to A4 (see Figures 9a and 9b).

That the LTECs for the gauges A1 to A4 (2 % Al_2O_3 PSZ) are lower than those for gauges B1 to B3 ("pure" PSZ), is quite reasonable, because the LTEC of the added Al_2O_3 is much less than that of PSZ, which is reported to be 5.30×10^{-6} K^{-1} at 20 °C [12].

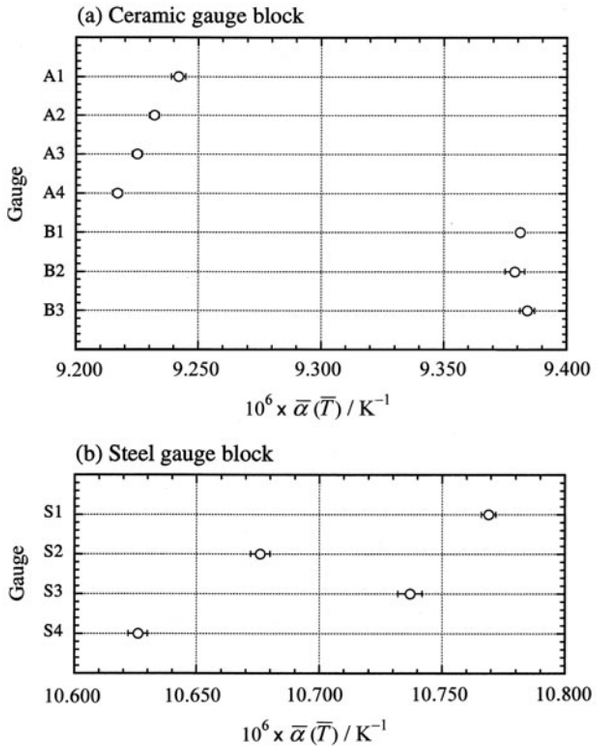

Figure 9. Linear thermal expansion coefficients at 20 °C for: (a) the two types of ceramic gauge block; (b) the steel gauge blocks. The uncertainty bars represent the standard deviation of the data points from the second-order polynomial fitting curve.

We calculated the LTEC for 2 % Al_2O_3 PSZ using Turner's equation [14]:

$$\alpha_r = (\alpha_1 F_1 K_1 \rho_2 + \alpha_2 F_2 K_2 \rho_1)/ (F_1 K_1 \rho_2 + F_2 K_2 \rho_1), \quad (4)$$

where α, F, K and ρ represent, respectively, LTEC, weight proportion, bulk modulus, and density. The subscripts 1 and 2 represent the two components, i.e. PSZ and Al_2O_3 in this case. The LTEC of the mixture was calculated using the physical constants and parameters for the two materials, listed in Table 5. The calculated result, $\alpha_r = 9.22 \times 10^{-6}$ K^{-1}, agrees extremely well with the measured LTEC for the 2 % Al_2O_3 PSZ gauge blocks: 9.23×10^{-6} K^{-1}.

The present measurements indicate that the LTECs of the ceramic gauges have very little scatter and suggest that reference values can be established for PSZ gauges. On the other hand, it may be difficult to define a reference value for the steel gauges, because their LTEC values show a much larger scatter, even though the gauges have the same nominal composition. In addition, the LTECs of commercially available steel gauges are well known to vary (sometimes by more than 1×10^{-6} K^{-1}) from gauge to gauge.

Table 5. Physical constants and parameters for PSZ and Al_2O_3 at 20 °C.

Physical constant/parameter	PSZ	Al_2O_3
α: LTEC ($\times 10^{-6}$ K^{-1})	9.38*	5.30**
F: weight proportion	0.98	0.02
K: bulk modulus ($\times 10^{11}$ Pa)	1.8***	2.3***
ρ: density ($\times 10^3$ kg/m^3)	6.0***	3.8***

*Present data.
**CODATA recommended value.
***From manufacturer's technical notes.

7. Summary

Ultra-high-precision linear thermal expansion coefficients (LTECs) of steel gauge blocks (four in all) and two kinds of partially stabilized zirconia (PSZ) gauge block (seven in all) were measured using an optical heterodyne interferometric dilatometer in the range –10 °C to 60 °C. The measurement system has a standard uncertainty of 1 nm in length measurement and 1 mK in temperature measurement, leading to a standard uncertainty of the order of 1×10^{-9} K^{-1} in the LTEC results. The degree of scatter of the measurements was found to be constant. The LTECs for all gauge blocks are described by a second-order polynomial function with respect to temperature (3), the coefficients of which are listed in Table 4.

The four gauge blocks A1 to A4 (2 % Al_2O_3 PSZ) showed LTECs in the range $(9.229 \pm 0.011) \times 10^{-6}$ K^{-1} at 20 °C. The intra-batch variability of the LTEC was estimated to be within $\pm 4 \times 10^{-9}$ K^{-1} from the results for gauges A3 and A4. The inter-batch variability was estimated to be at most 25×10^{-9} K^{-1} from the results for gauges A1 to A4. The LTECs of gauges B1 to B3 (99.9 % PSZ) were $(9.381 \pm 0.003) \times 10^{-6}$ K^{-1} at 20 °C. The intra-batch variability of the LTECs for these gauges was the same as that for gauges A3 and A4. Compared with the ceramic gauge blocks, the LTECs of the steel gauges, S1 to S4, showed much larger scatters, of up to 0.14×10^{-6} K^{-1}. The LTECs for the steel blocks were $(10.702 \pm 0.064) \times 10^{-6}$ K^{-1} at 20 °C. The difference between the LTECs of the two kinds of ceramic gauge block, 2 % Al_2O_3 PSZ and 99.9 % PSZ, can readily be calculated using Turner's equation.

Acknowledgements. We greatly appreciate the helpful suggestions of Dr Katuo Seta of the NRLM, and Mr M. Ueda and Mr S. Shutoh of the Mitutoyo Corporation, in carrying out this work.

References

1. Bennett S. J., *Metrol. Insp.,* 1978, **10**(5), 35, 37.
2. Debler E., Bohme H., *Feinwerktech. Messtech.*, 1980, **88**(1), 27-30 (in German).

3. Hughes E. B., *Proc. SPIE – Int. Soc. Opt. Eng. (USA)*, 1994, **2088**, 179-189.
4. Wen-Mei Hou, Thalmann R., *Proc. SPIE – Int. Soc. Opt. Eng. (USA)*, 1998, **3477**, 272-278.
5. Vaucher B. G., Thalmann R., Baechler H., *Metrologia*, 1995, **32**, 79-86.
6. Darnedde H., Helmcke J., *Metrologia*, 1996, **33**, 485-491.
7. Okaji M., Yamada N., *High Temp.-High Press.*, 1997, **29**(1), 89-95.
8. Okaji M., Yamada N., *Thermal Conductivity 24/Thermal Expansion 12*, 1999, 336-343.
9. Kirby R. K., Hahn T. A., Natl. Bur. Stand. Certificate, Standard Reference Material 736, Copper – Thermal Expansion, 1969.
10. Kirby R. K., Hahn T. A., Natl. Bur. Stand. Certificate, Standard Reference Material 737, Tungsten – Thermal Expansion, 1976.
11. Kirby R. K., Hahn T. A., Natl. Bur. Stand. Certificate, Standard Reference Material 739, Fused Silica – Thermal Expansion, 1971.
12. Swenson C. A., Roberts R. B., White G. K., *CODATA Bulletin*, 1985, **59**, 13-18.
13. Okaji M., Birch K. P., *Metrologia*, 1991, **28**, 27-32.
14. Turner P. S., *J. Res. Natl. Bur. Stand.*, 1946, **37**, 239.

Received on 10 August 1999 and in revised form on 30 September 1999.